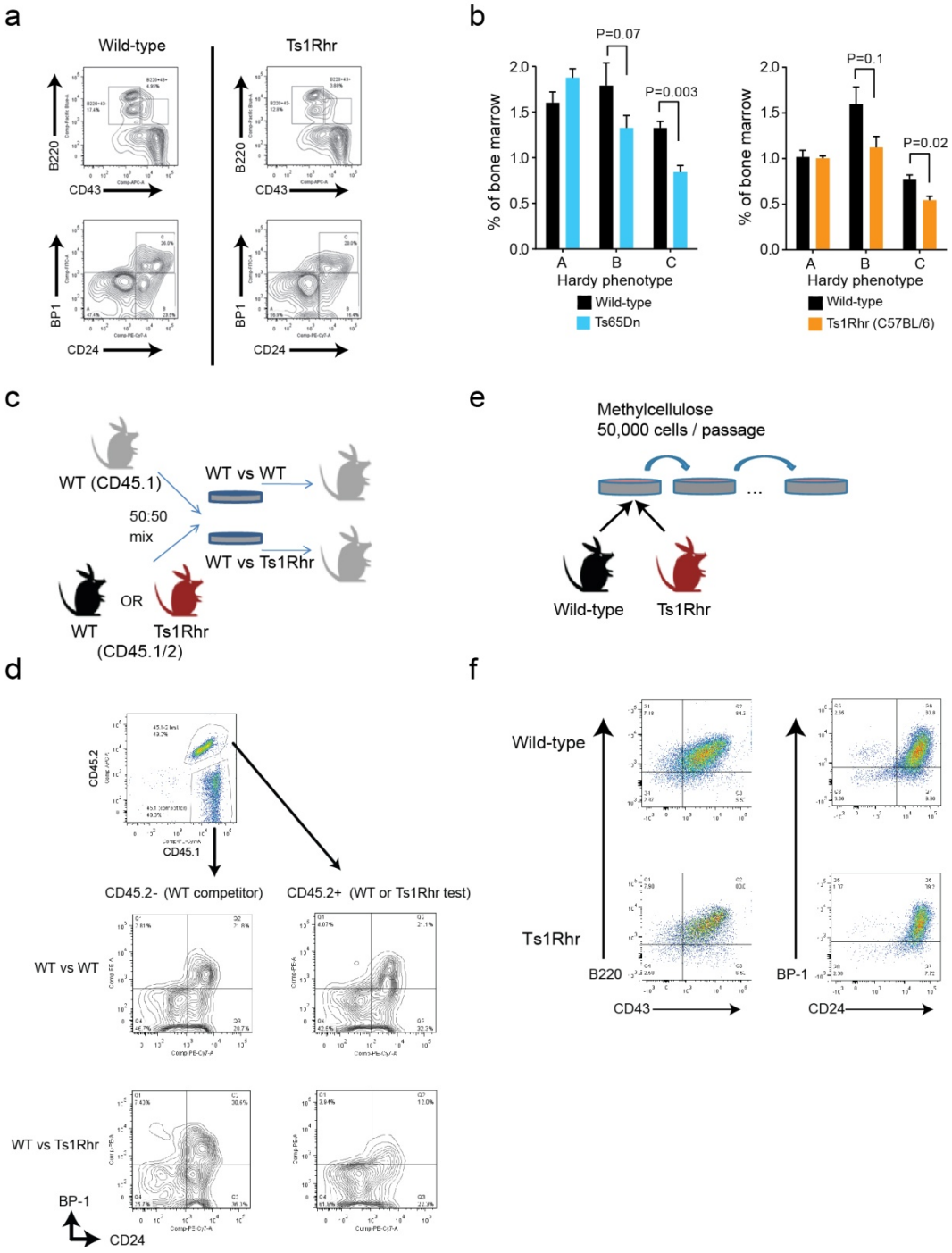

Supplementary Figure 1. Abnormal differentiation *in vivo* and colony growth *in vitro* of B cells with triplication of chr.21 orthologs.

(a) (Top) B220 and CD43 staining of bone marrow from Ts1Rhr and wild-type mice, highlighting the more immature B220+CD43+ and more mature B220+CD43- B cell populations. (Bottom) CD24 and BP1 staining of the B220+CD43+ subpopulation demonstrates the early Hardy fractions: A (CD24-BP1-), B (CD24+BP1-), and C (CD24+BP1+). (b) Hardy subfractions of the B220+CD43+ population as absolute percentages of bone marrow mononuclear cells by flow cytometry from Ts65Dn (blue) or

C57BL/6 Ts1Rhr (orange) animals compared to wild-type littermate (black) mice (n=4 mice per genotype). (c) Schematic for the competitive bone marrow transplantation assay. (d) Representative Hardy fraction staining in bone marrow gated on CD45.2 negative (left) competitor cells or CD45.2 positive (right) test cells. The top rows are wild-type test cells, and the bottom rows are Ts1Rhr test cells. There are fewer Ts1Rhr Hardy B/C cells and greater numbers of Ts1Rhr Hardy A cells in recipients of wild-type:Ts1Rhr competitive transplants (bottom right). (e) Schematic of the methylcelluose replating assay. Whole BM from Ts1Rhr or wild-type mice was plated in semi-solid medium containing cytokines favoring B cell or myeloid colony growth. 50,000 cells were collected from pooled colonies every seven days and replated in fresh media. (f) Cell surface phenotype of passage 1 B cell colonies from Ts1Rhr and wild-type animals is similar. Representative flow cytometry plots of Hardy fraction cell surface phenotype of passage 1 Ts1Rhr and wild-type B cell colonies is shown. All cells are also B220+CD43+ (not shown).

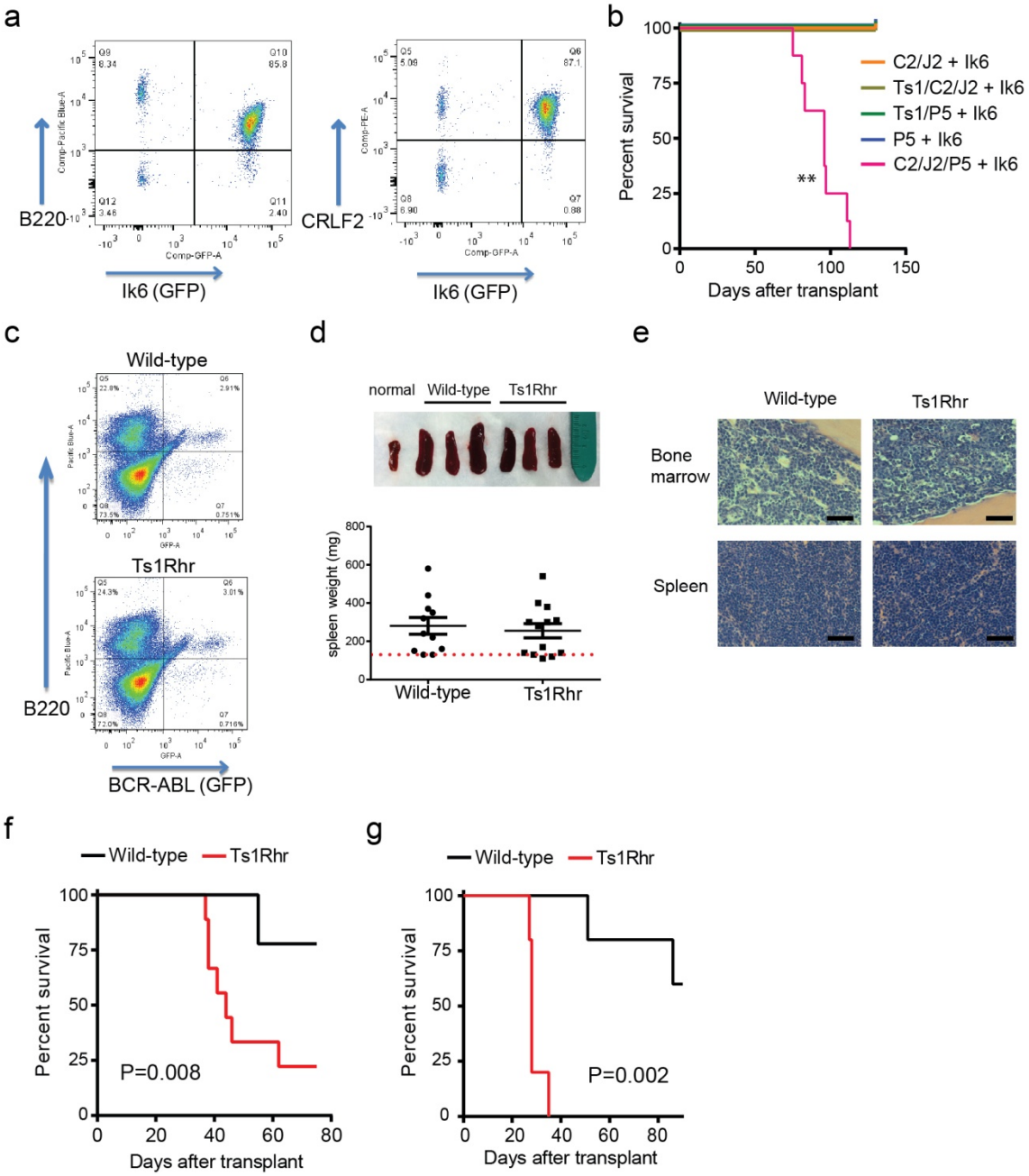

Supplementary Figure 2. Characterization of the B-ALL that arises in Ts1Rhr bone marrow.
(a) Representative phenotype of C2/J2/P5/Ts1 + Ik6 B-ALL is shown, demonstrating expression of human CRLF2 in the leukemic B cells that also co-express dominant negative Ikaros (Ik6). (b) Leukemia-free survival for wild-type mice after transplantation with bone marrow of the genotypes listed transduced with dominant negative Ikaros (Ik6) (n=6-8 mice/group, **P<0.01 for C2/J2/P5 + Ik6 versus any other genotype by log-rank test). (c) Transduced Ts1Rhr and wild-type bone marrow is shown using flow cytometry for B220 and GFP (BCR-ABL) demonstrating approximately equal proportions of GFP+ cells at the time of transplantation. (d) Ts1Rhr and wild-type BCR-ABL B-ALLs demonstrate similar splenomegaly at the time of death with leukemia. Red dotted line represents upper limit of normal spleen weight. (e) Bone marrow and spleen histology by hematoxylin and eosin staining shows similar infiltration with B-ALL cells in Ts1Rhr and wild-type B-ALLs (scale bar = 50 μm). (f) Survival curves

for recipients of Ts1Rhr or wild-type bone marrow cells (on a C57BL/6 background) transduced with BCR-ABL (n=9 mice per group, curves compared by log-rank test). (g) Increase in B-ALL from Ts1Rhr bone marrow is progenitor B cell autonomous. Hardy B cells were sorted from Ts1Rhr or wild-type bone marrow, transduced with BCR-ABL, and equal numbers of cells were transplanted into wild-type recipients. (n=5 mice per group, curves compared by log-rank test).

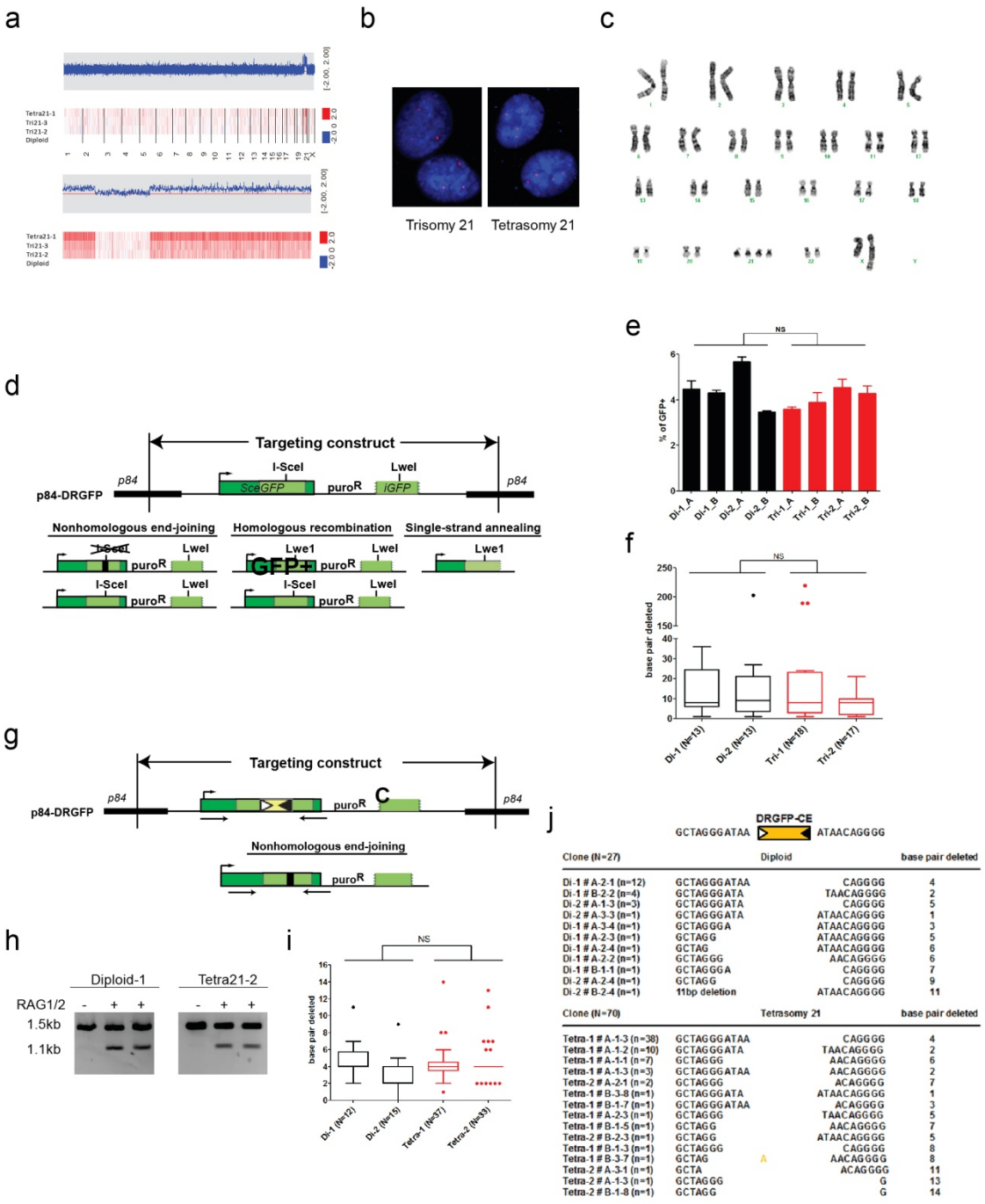

Supplementary Figure 3. Trisomy and tetrasomy 21 retinal pigment epithelium (RPE) cells generated by microcell-mediated chromosome transfer (MMCT) do not have differences in DNA repair after I-SceI or RAG-induced cleavage.

(a) Single nucleotide polymorphism (SNP) array data for a tetrasomy 21 RPE clone (tetra 21-1), two trisomy 21 (tri21-2 and tri21-3) clones, and a diploid clone are shown across the entire genome (top) or chromosome 21 (bottom). (b) Representative fluorescence *in situ* hybridization for human chr.21 in trisomy 21 and tetrasomy 21 RPE cells (red = chr.21 probe, blue = DAPI). (c) Representative G-banding karyotype for a tetrasomy 21 RPE cell line. (d) The DR-GFP construct was targeted to the *p84* locus in

RPE cells containing 2 or more copies of chr.21. A single double-strand DNA break induced by I-SceI can be repaired by multiple pathways. (e) Repair after I-SceI cleavage in cells lacking classical nonhomologous end-joining (NHEJ) factors (e.g. KU70/80, XRCC4/LIG4) is characterized by higher rates of homologous recombination and more extensive deletions at NHEJ junctions (Pierce et al. *Genes Dev* 15:3237-42). However, the frequencies of homologous recombination (shown as percent GFP-positive) induced by I-SceI do not significantly differ between disomic (Di) and trisomy 21 (Tri) RPE clones. Two clones from each genotype were assayed on two occasions in triplicate. (f) Similarly, the phenotype of nonhomologous end-joining induced by I-SceI did not significantly differ between disomic and trisomy 21 RPE clones. The number of base pairs deleted at junctions formed by NHEJ from two clones from each genotype is shown. (g) The DR-GFP-CE construct targeted to the *p84* locus can be used to assess repair after RAG cleavage. Cleavage at the paired RAG recognition signal sequences (white and black triangles) results in removal of the intervening sequence (in yellow) and nonhomologous end joining (NHEJ) between the double-strand break ends. (h) PCR shows no difference in the frequencies of the RAG-induced deletion between diploid and tetrasomy 21 cells. Two biologic replicates are shown for each genotype. (i) Repair junctions after RAG cleavage in cells lacking classical NHEJ factors (e.g. KU70/80, XRCC4/LIG4) typically have longer deletions and more extensive use of short stretches of homology than in wild-type cells (Weinstock et al. *Mol Cell Biol* 26:131-9). However, the number of base pairs deleted after cleavage by RAG and NHEJ did not significantly differ between disomic and tetrasomy 21 cells (n=2 clones per genotype). (j) The junction sequences are shown for disomic (n=27) and tetrasomy 21 (n=70) RPE clones. A single nucleotide insertion is shown in Tetra-1 # B-3-7 (yellow).

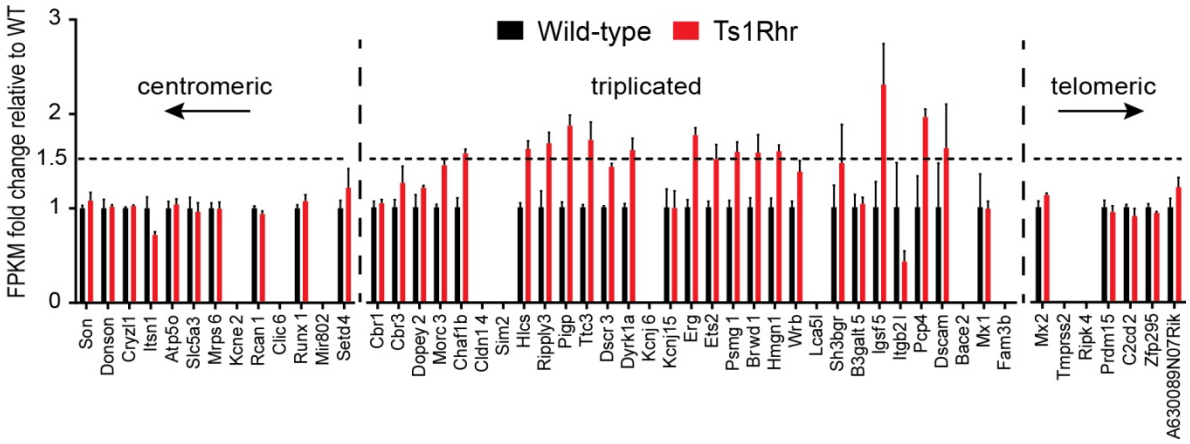

Supplementary Figure 4. RNA-seq expression of the triplicated genes in Ts1Rhr compared to wild-type B cells.

RNA sequencing of Ts1Rhr and wild-type B cells (n=3 mice per genotype) showing relative expression levels among the 25 expressed triplicated genes (absolute fragments per kilobase per million reads [FPKM] > 0.1), and the flanking centromeric and telomeric regions.

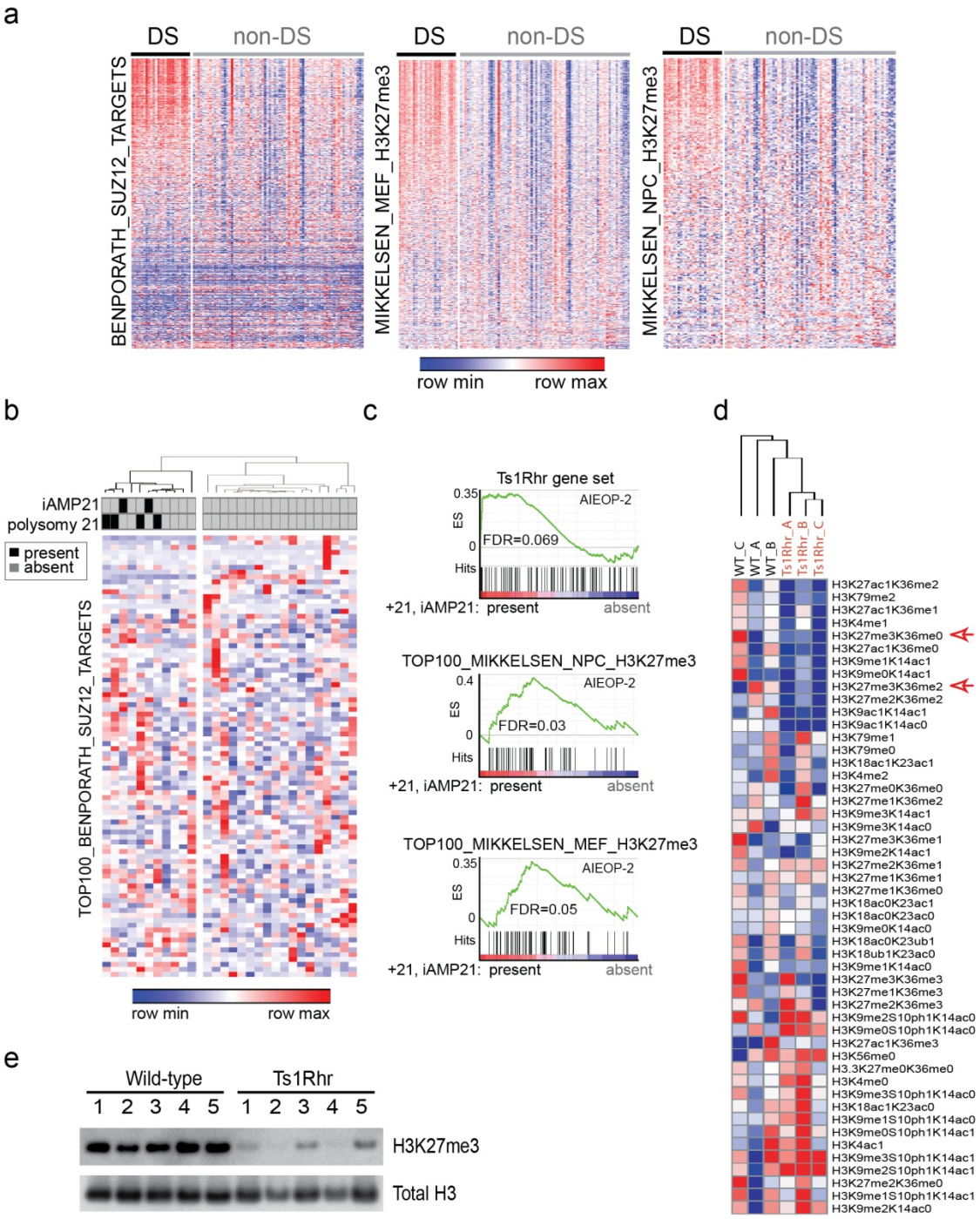

Supplementary Figure 5. Down sydrome-ALL is associated with overexpression of PRC2 targets and genes marked by H3K27me3, Ts1Rhr and PRC2/H3K27me3 gene signatures distinguish non-Down sydnrome-ALL with somatic gain of chromosome 21 or iAMP21, and Ts1Rhr B-ALLs are associated with H3K27 hypomethylation.

(a) Heat maps of all genes comprising three of the top five scoring target gene sets enriched in the core Ts1Rhr signature in Down syndrome-ALLs and non-Down syndrome-ALLs. (b) Unsupervised clustering of a validation cohort of 30 non-Down syndrome pediatric B-ALL gene expression signatures (the AIEOP-2 cohort) is shown using a 100-gene SUZ12 target gene set. Four patients with somatic gain of

chr.21 and two with iAMP21 cluster within a distinct group with 5 additional cases (P=0.001 by Fisher's exact test). (c) GSEA plots of the Ts1Rhr gene set and the top 100 discriminating genes in the Mikkelsen NPC and MEF H3K27me3 gene sets from the AIEOP cohort, queried in the primary human B-ALLs in the AIEOP-2 cohort containing cases with somatic +21 and iAMP21. ES indicates enrichment score. (d) Unsupervised hierarchical clustering of histone H3 post-translational modifications in splenocytes from mice with Ts1Rhr and wild-type BCR-ABL B-ALLs quantitated by mass spectrometry (blue-red = low-to-high relative amount of each listed peptide, n=3 independent leukemias for each genotype). Peptides containing H3K27me3 with lower abundance in Ts1Rhr B-ALLs are indicated by arrows. (e) Western blotting in sorted CD19+ Ts1Rhr and wild-type B-ALLs (n=5 independent leukemias for each genotype, distinct from those in panel D).

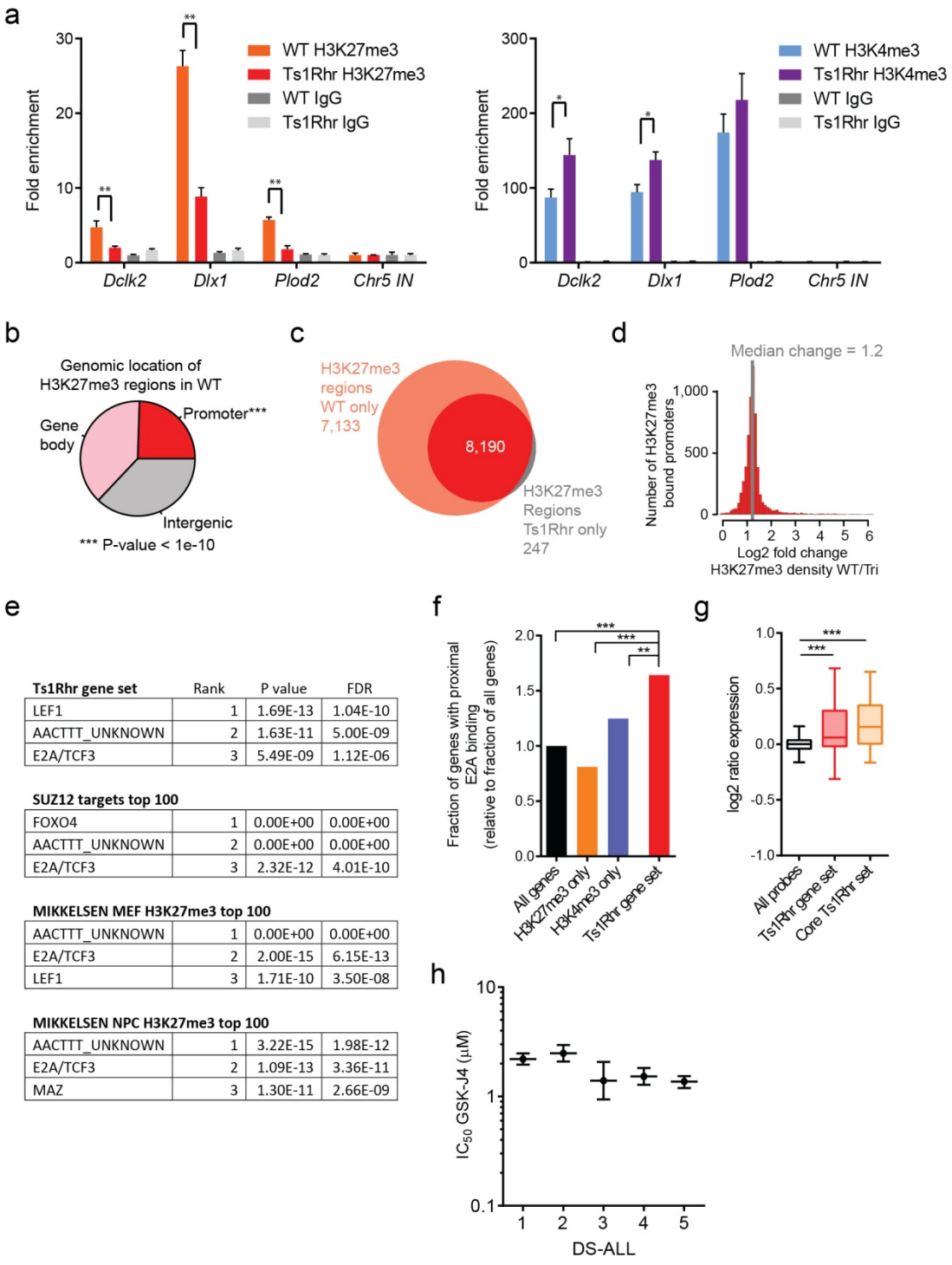

Ts1Rhr gene set	Rank	P value	FDR
LEF1	1	1.69E-13	1.04E-10
AACTTT_UNKNOWN	2	1.63E-11	5.00E-09
E2A/TCF3	3	5.49E-09	1.12E-06

SUZ12 targets top 100			
FOXO4	1	0.00E+00	0.00E+00
AACTTT_UNKNOWN	2	0.00E+00	0.00E+00
E2A/TCF3	3	2.32E-12	4.01E-10

MIKKELSEN MEF H3K27me3 top 100			
AACTTT_UNKNOWN	1	0.00E+00	0.00E+00
E2A/TCF3	2	2.00E-15	6.15E-13
LEF1	3	1.71E-10	3.50E-08

MIKKELSEN NPC H3K27me3 top 100			
AACTTT_UNKNOWN	1	3.22E-15	1.98E-12
E2A/TCF3	2	1.09E-13	3.36E-11
MAZ	3	1.30E-11	2.66E-09

Supplementary Figure 6. ChIP-seq and CHIP-qPCR show decreased H3K27me3 at promoters in Ts1Rhr B cells, the Ts1Rhr gene set is enriched for E2A/TCF3 and LEF1 targets, and Down syndrome-ALLs are sensitive to GSK-J4.

(a) ChIP for H3K27me3 (left), H3K27me3 (right), or control rabbit IgG followed by quantitative PCR on a representative set of genes from the Ts1Rhr signature in an independent validation set of wild-type and Ts1Rhr mice (n=3 mice per genotype, one representative of two independent experiments). Data represented as fold enrichment over input relative to a negative control intergenic region on chr.5 (Chr 5

IN) (**P<0.01, *P<0.05). (b) H3K27me3 enriched regions in wild-type B cells. The promoter region is defined as the 5kb flanking annotated transcription start sites. Overlap of H3K27me3 regions with the promoter region was significant in comparison to a random background model of the genome ($P<10^{-10}$). (c) Venn diagram showing the number and overlap between H3K27me3 enriched regions in wild-type (WT) or Ts1Rhr B cells. (d) The $\log_2$ fold difference in density of H3K27me3 at promoters between Ts1Rhr and wild-type B cells is shown. (e) Top three ranked transcription factors with predicted binding sites among promoters of genes in the listed sets as queried in MSigDB "c3.tft" defined in the TRANSFAC database (version 7.4, www.gene-regulation.com). (f) Relative fraction of genes that have proximal E2A/TCF3 occupancy among all genes (7129 of 20671), genes with only H3K27me3 (557 of 1994) or H3K4me3 (4032 of 9360) at the promoter in wild-type B cells, or genes in the Ts1Rhr gene set (85 of 150) (**P<0.01, ***P<0.0001 versus the Ts1Rhr gene set by Chi-square with Yates' correction). (g) Expression of genes in the Ts1Rhr and Core Ts1Rhr sets are increased compared to all probesets in wild-type B cell progenitors as compared to *E2A*$^{-/-}$ (expression data from Lin YC et al. *Nature Immunology* 11:635-43; ***P<0.0001 by Student t-test, center bars = median, box = 25-75% confidence interval, whiskers = 10-90% confidence interval). (h) IC_{50} for five Down syndrome-ALLs treated *in vitro* with GSK-J4 (error bars represent 95% confidence intervals).

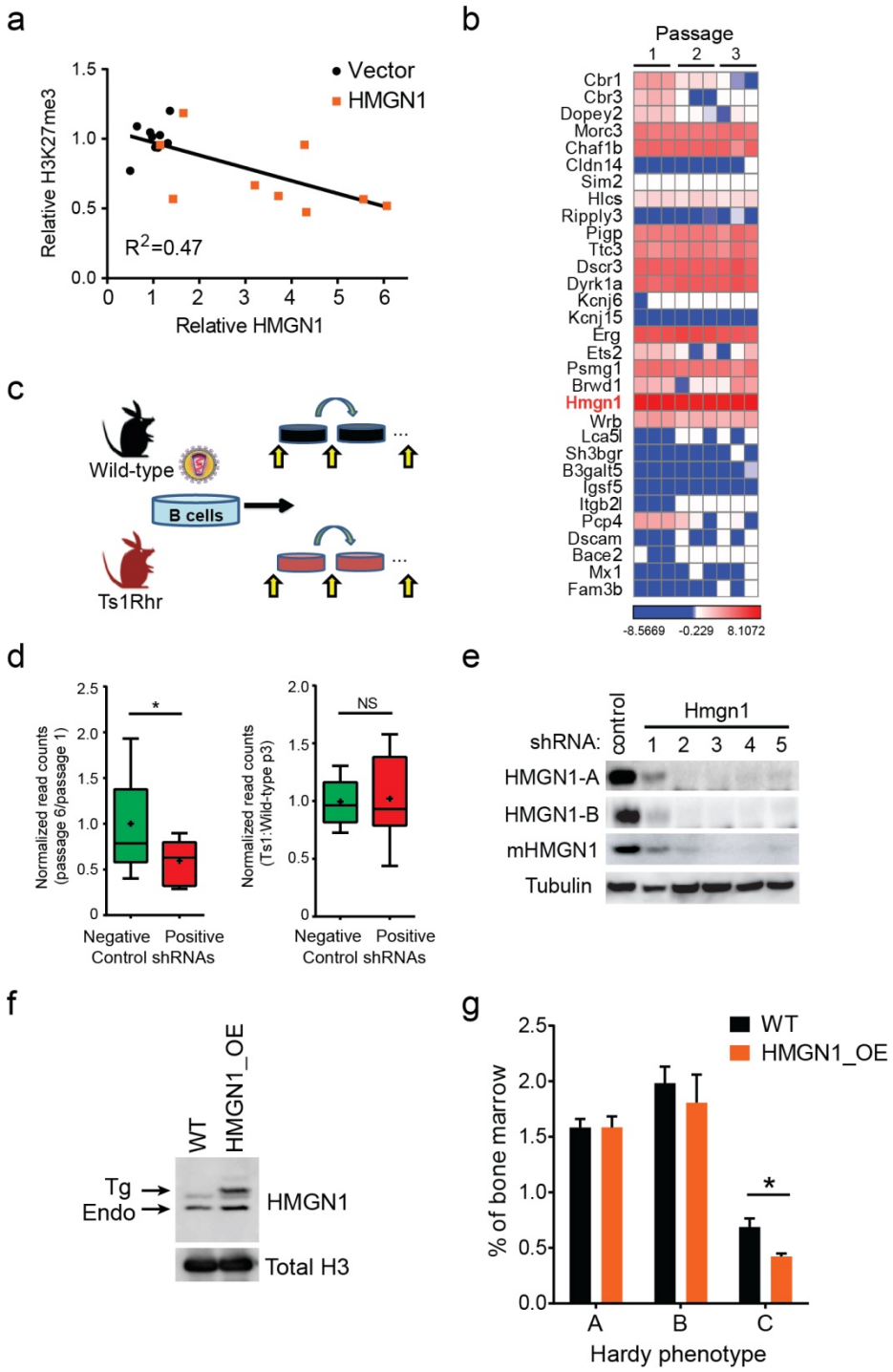

Supplementary Figure 7. HMGN1 overexpression alone results in multiple B cell phenotypes observed with triplication of the entire 21q22 orthologous region.

(a) Relative quantitation of H3K27me3 and HMGN1 in BaF3 lymphoblasts transduced with empty vector of mouse HMGN1. (b) Heatmap showing RNA expression of the 31 triplicated genes in passages 1, 3, and 6 in triplicate Ts1Rhr cultures (blue-red = low to high $\log_2$ FPKM values, genes listed in genomic order). (c) Schematic of the primary B cell shRNA experiment. Passage 1 B cells from Ts1Rhr or wild-type bone marrow were pooled after infection with individual lentiviral shRNAs targeting either a

triplicated gene (5 shRNA/gene) or a control (n=30). DNA was collected post-infection (baseline) and after each passage (indicated by arrows), and the relative representation of each shRNA was quantitated by next generation sequencing. Data represent the average of independent biological replicates from wild-type (n=3) and Ts1Rhr (n=4) animals. (d) Normalized quantitation of negative (non-targeting) and positive (known to be toxic) control shRNAs in passage 6 Ts1Rhr colonies relative to input (left) demonstrates preferential loss of positive control shRNAs. Neither positive nor negative control shRNAs were preferentially lost from Ts1Rhr passage 3 cells compared to wild-type (right, Tukey box and whiskers plots, horizontal bar is the median and plus is the mean; *P<0.05; NS, not significant). (e) Western blotting in BaF3 lymphoblasts confirming knockdown of HMGN1. Antibodies are: A (Abcam), B (Aviva), mHMGN1 (affinity purified murine HMGN1 antibody). (f) Western blotting of HMGN1 in B cell colonies from wild-type and HMGN_OE mice using the Abcam HMGN1 antibody. “Endo” represents endogenous mouse HMGN1 and “Tg” represents transgenic human HMGN1. (g) Hardy B cell subfractions as percentages of bone marrow cells from wild-type (black) and HMGN1_OE (orange) littermates (n=4 per group, *P<0.05).

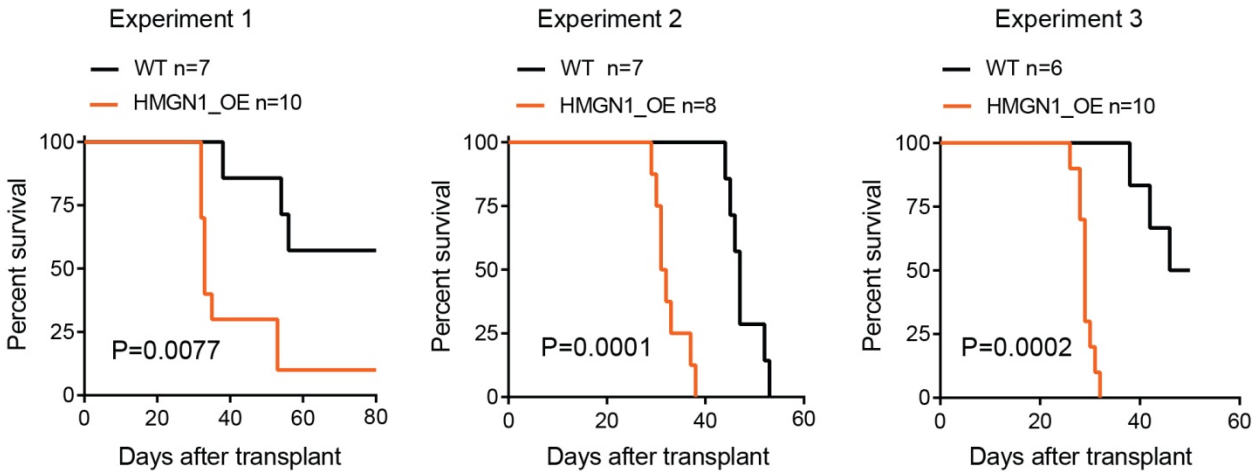

Supplementary Figure 8. HMGN1 overexpression cooperates with BCR-ABL to promote B-ALL *in vivo*.
Results from three independent experiments showing leukemia-free survival of recipients of wild-type (WT) or HMGN1 overexpressing (HMGN1_OE) bone marrow transduced with BCR-ABL (curves compared by log-rank test).